Thin Solid Films 548 (2013) 255–258

Contents lists available at ScienceDirect

Thin Solid Films

journal homepage: www.elsevier.com/locate/tsf

Synthesis and characterization of thin film electroluminescent devices all-prepared by ultrasonic spray pyrolysis

E.B. Ramírez [a], M. Bizarro [b], J.C. Alonso [b,*]

[a] Universidad Autónoma de la Ciudad de México, Calle Prolongación San Isidro Núm. 151, Col. San Lorenzo Tezonco, Iztapalapa 09790, D. F., México, Mexico
[b] Instituto de Investigaciones en Materiales, Universidad Nacional Autónoma de México, Apartado Postal 70-360, Coyoacán 04510, Distrito Federal, México, Mexico

ARTICLE INFO

Article history:
Received 6 April 2013
Received in revised form 26 September 2013
Accepted 2 October 2013
Available online 11 October 2013

Keywords:
ACTFEL device
Ultrasonic spray pyrolysis
Electroluminescence
ZnS:Mn

ABSTRACT

Alternating current thin film electroluminescent devices have been fabricated using aluminum-doped zinc oxide (ZnO:Al) as transparent conducting layer, aluminum oxide (Al_2O_3) as insulating layers, and manganese-doped zinc sulfide (ZnS:Mn) as electroluminescent layer. All these films were deposited by the ultrasonic spray pyrolysis technique at the same temperature (450°) on glass substrates, forming a standard MISIM (metal–insulator–semiconductor–insulator–metal) configuration. The electroluminescence of MISIM devices with a total thickness of ~1330 nm was investigated by applying a sinusoidal voltage with a frequency of 10 kHz. The devices showed orange-emission spectra centered at approximately 570 nm, characteristic of $^4T_1 \rightarrow {}^6A_1$ radiative transitions of Mn^{2+} ions in the ZnS host, with a sharp intensity increase upon increasing the root mean square voltage above a threshold of 25 V and a rapid saturation for voltages higher than 38 V. The electroluminescent emission of these MISIM structures can be observed with the naked eye under ambient illumination.

1. Introduction

Although at present there are many technologies for the fabrication of flat panel displays, such as liquid crystals, plasmas, field emission displays, and organic light emitting diodes, alternating current thin film electroluminescent (ACTFEL) devices continue being of interest because they offer several advantages compared to other types of flat panel displays, such as: complete solid state nature and hardness, lightweight, high transparency and high luminance [1–4]. A typical ACTFEL device consists of a MISIM multilayer structure, which is usually deposited on a transparent glass substrate. In the standard MISIM configuration the bottom electrode (M) is a transparent conducting layer deposited on the glass substrate, then the bottom insulating layer (I), the semiconducting (S) "phosphor" layer, and the top insulating (I) layers are deposited, and finally, a top reflecting electrode (M). There is a wide variety of materials and deposition techniques that have been used for preparing the layers incorporated in a MISIM structure. The most common transparent electrode material used in a standard ACTFEL is indium tin oxide (ITO), however many other transparent conducting oxides (TCO) such as SnO_2: (Sb, F, As, Nb, Ta), and ZnO: (Al, In, Ga, F), etc. have also been used [1,5,6]. Due to its high luminescence and its isovalent nature, which leads to more ideal ACTFEL device operation, ZnS:Mn has been the most common "phosphor" layer used for commercial, research and development ACTFELs [7]. The techniques more used for depositing these ZnS:Mn layers have been: sputtering [4,8–10], electron-beam evaporation [11–13], and thermal evaporation [14–16]. With the purpose of fabricating multicolor or full color ACTFEL devices, other oxide-based and sulfide-based materials, prepared by sputtering, electron beam and thermal evaporation, have also been investigated [2,3,15,17]. With respect to the insulating layers used for ACTFEL devices, which must meet the stringent requirements of having high dielectric constant and high electric field strength [1], although Y_2O_3 prepared by sputtering and electron-beam evaporation has been extensively used [3,4,9,13,15], many other insulators prepared by the same techniques, such as: Sm_2O_3, Eu_2O_3, MgF_2, AlTiO, SiO_2, Al_2O_3 and HfO_2 have been investigated [1–3,8,12,14,18].

In this work we report the preparation of MISIM-ACTFEL devices using films of: ZnO:Al as TCO layer, Al_2O_3 as insulating layers, and ZnS:Mn as phosphor layer, all-prepared by the ultrasonic spray pyrolysis technique, which has the advantage of simplifying and reducing costs of fabrication, because this technique is relatively simple and it does not require vacuum systems. The spray pyrolysis technique, in the pneumatic version, has been previously used for preparing ZnS:Mn luminescent films [19], and these films have been used in ACTFEL devices fabricated with SnO_2:Sb deposited by RF sputtering as TCO layer, and SiO_2 deposited by plasma enhanced chemical vapor deposition as insulating layers [20]. ZnS:Tb,Ag films deposited by pneumatic spray pyrolysis have also been used in ACTFEL devices [21]. ZnO:Al films with adequate properties as TCO layers have been recently deposited by pneumatic spray pyrolysis [22–24]. On the other hand, Al_2O_3 films with violet-blue photoluminescence [25] or with good insulating properties [26,27] have been prepared by the ultrasonic spray pyrolysis technique. Based on these previous works, we were motivated to fabricate and characterize ACTFEL devices, in which all the stacked

* Corresponding author.
E-mail address: alonso@unam.mx (J.C. Alonso).

0040-6090/$ – see front matter © 2013 Elsevier B.V. All rights reserved.
http://dx.doi.org/10.1016/j.tsf.2013.10.003

films (ZnO:Al/Al_2O_3/ZnS:Mn/Al_2O_3) were deposited by the ultrasonic spray pyrolysis technique.

2. Experimental details

The schematic illustration of our MISIM devices is shown in Fig. 1 All the thin films conforming the MISIM structures were deposited by the ultrasonic spray pyrolysis technique at atmospheric pressure and at substrate temperature of 450 °C. The substrates were 2.5 × 1.5 cm^2 corning glass slices, which were ultrasonically cleaned with trichloroethylene, acetone and methanol, before film deposition. With this cleaning procedure the films exhibited good adherence to the substrates and to the preceding films. The start solution used for depositing the transparent conducting film of aluminum doped zinc oxide (ZnO:Al) was made with 0.2 mol/l zinc acetate dehydrate ($Zn(CH_3COO)_2$ $2H_2O$) and 5 at.% of aluminum acetilacetonate ($Al(C_5H_7O_2)_3$) with respect to the zinc acetate, diluted with 8.5 parts of anhydrous methanol and 1 part of deionized water and 1 ml of acetic acid. The precursor solution for depositing the insulating films of Al_2O_3, was made with 0.05 mol/l of aluminum acetilacetonate diluted into 1 part of anhydrous methanol, 3 parts of deionized water and 3 ml of acetic acid. The active layer of ZnS:Mn was deposited from a precursor solution prepared with 0.033 mol/l of zinc acetate dehydrate $C_4H_6O_4Zn2H_2O$, 0.033 mol/l of 1,3-dimethyl-2-thiourea $CH_3NHCSNHCH_3$ and 5 at.% of manganese (II) chloride reagent $MnCl_24H_2O$, diluted with 1 part of isopropyl alcohol and 1 part of deionized water and 3 ml acetic acid. All the precursor solutions were mixed at room temperature for 10 min with a magnetic stirrer, at the rate of 120 rpm, and they were not heated at all during deposition. Clear and transparent solutions were obtained after the stirring process. An experimental set up similar to that shown in reference [28] was used. In this system, the aerosol generated by the ultrasonic nebulizer is conveyed by a carrier or transport gas toward the deposition zone (deposition chamber at atmospheric pressure), where it pyrolyzes on the heated substrate. This system also allows us to introduce a director gas at the top of the deposition zone for increasing the velocity of the droplets arriving on the heated substrate, without altering the flow rate of the aerosol carrier gas. The carrier and director gases were air for all the deposits, whose flow rates were constant and fixed at 3.5 l/min and 1.5 l/min, respectively. The first thin film deposited over the glass substrate was the transparent conducting contact (electrode 1) of ZnO:Al. This film was deposited during 10 min at a deposition rate of ~100 nm/min, giving a final thickness of ~1000 nm. The thickness of each insulating film of Al_2O_3 was ~90 nm, with a deposition rate of ~13 nm/min, and a deposition time of 7 min. The thickness of the emitting ZnS:Mn layer sandwiched between the two Al_2O_3 insulating layers, was ~150 nm. In this case the deposition rate and time were ~12.5 nm/min and 12 min, respectively.

A pattern of circular dots of aluminum (Al) electrodes with diameters ~1.15 mm and thickness of ~200 nm were deposited by thermal evaporation through a metallic mask onto the top insulating Al_2O_3 film. This pattern defined an arrangement of ~6 × 4 = 24 electroluminescent devices per substrate with circular emitting areas of around 1.04 mm^2. The electroluminescent (EL) emission characteristics of these devices were investigated by applying sinusoidal voltages with a frequency of 10 kHz. The EL signal was collected using a quartz optical fiber, and measured in the range from 450 to 700 nm with a Spex-Fluoromax spectrometer. The root mean square (RMS) voltages applied to register the electroluminescent spectra of the devices, in the entire operation region from threshold to saturation, were: 25, 32, 38, 42, 51 and 67 V. The crystalline structure of the luminescent ZnS:Mn film was determined by X-ray diffraction measurements using a SIEMENS D500 difractometer, with an X-ray source of Cu K_α, line (0.15406 nm), at an incidence angle of 1° (grazing beam configuration).

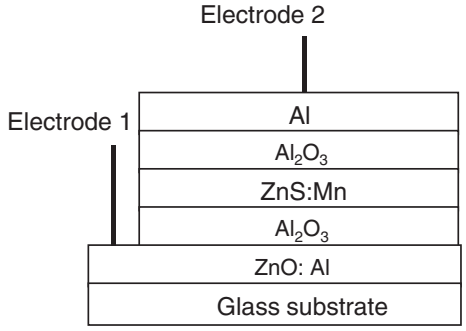

Fig. 1. Schematic illustration of the MISIM structure.

3. Results and discussion

According to the X-ray diffraction pattern shown in Fig. 2, the ZnS:Mn film used in the MISIM structures, was polycrystalline, where the main diffraction peak at 2θ = 28.49° and the other smaller peaks located at 26.82°, 30.45°, 39.61°, 47.57, 51.75° and 56.39° were identified to originate from the (002), (100), (101), (102), (110), (103) and (112) planes of the hexagonal wurzite phase of ZnS, respectively. Information on the crystallite sizes was obtained from the full widths at half maximum of the diffraction peaks, using the Scherrer equation, without considering stress or other effects, and the sizes were in the range from ~31 nm to ~62 nm.

Fig. 3 shows a typical photoluminescence (PL) spectrum of a ZnS:Mn phosphor layer with an excitation wavelength of 325 nm from the xenon lamp of the Spex-Fluoromax spectrometer, along with the electroluminescent (EL) emission spectrum of the MISIM structure incorporating this ZnS:Mn film, obtained with an amplitude of the exciting voltage of V(RMS) = 42 V. Both, PL and EL spectra show only a peak centered at ~573 nm which can be associated with the characteristic $^4T_1 \rightarrow {}^6A_1$ emission of Mn^{2+} ions in the ZnS host [29]. Although the wavelength position of this peak varies in the range from 572 nm to 600 nm, depending on the crystalline phase, or whether this material is in the form of bulk, thin film, nanoparticles or nanocrystals, the existence of stress, excitation wavelength, Mn concentration, etc., at present it is not clear how this position depends on all these aspects [16,19,29–33].

The EL spectra of MISIM structures were obtained for different RMS voltages. Fig. 4 shows the typical EL spectra of a MISIM structure with a whole thickness of ~1330 nm [ZnO:Al (1000 nm)/Al_2O_3 (90 nm)/ZnS:Mn (150 nm)/Al_2O_3 (90 nm)], for the threshold voltage V1 = 25 V, and V2 = 32 V, meanwhile Fig. 5 shows the EL spectra of the same MISIM structure for the higher applied voltages of V3 = 38 V, V4 = 42 V,

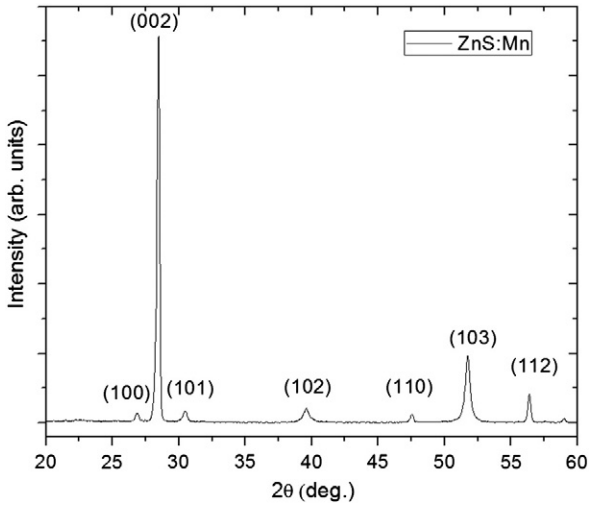

Fig. 2. X-ray diffraction pattern of the ZnS:Mn phosphor layer used in the MISIM structures prepared by ultrasonic spray pyrolysis.

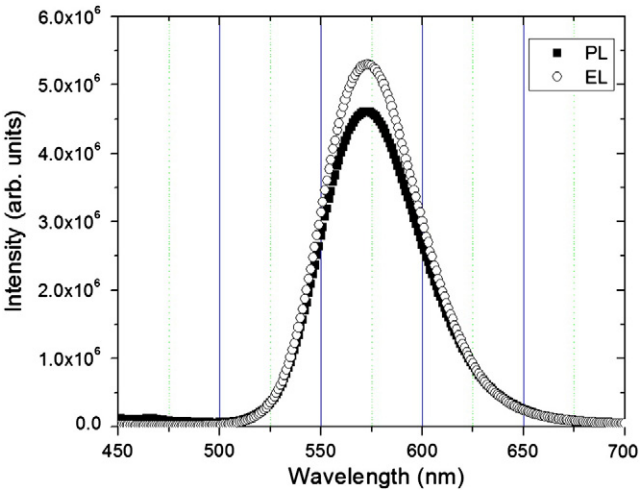

Fig. 3. Typical PL ■ and EL ○ spectra of the ZnS:Mn film and the MISIM structure with ZnS:Mn film as a phosphor layer prepared by ultrasonic spray pyrolysis. In this case the EL spectrum of the MISIM structure was obtained at 42 V (RMS).

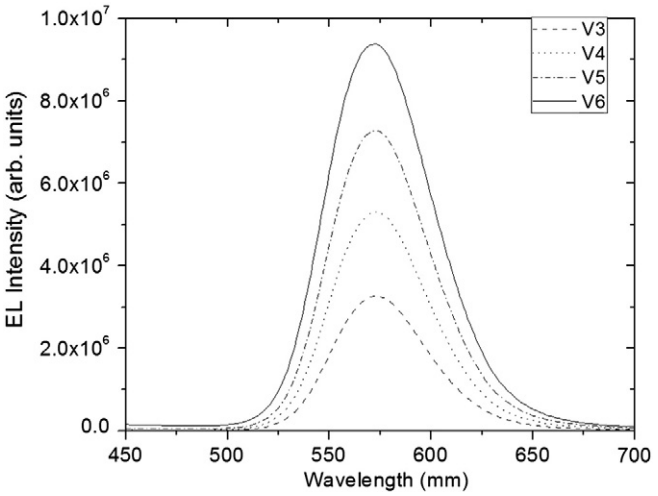

Fig. 5. EL spectra the MISIM structure prepared by ultrasonic spray pyrolysis, with ZnS:Mn film as a phosphor layer, for the RMS voltages: V3 = 38 V, V4 = 42 V, V5 = 51 V, and V6 = 67 V. The intense of the peak is 3.3×10^6 (a.u.), 5.3×10^6 (a.u.), 7.3×10^6 (a.u.), and 9.3×10^6 (a.u.), respectively.

V5 = 51 V, and V6 = 67 V. As can be seen from Fig. 4 the peak EL intensity increases by one order of magnitude as the applied voltage increases from the threshold voltage V1 to V2. Then as Fig. 5 shows, for the applied voltage V3 the peak EL intensity increases by two orders of magnitude compared with that obtained with the previous voltage V2, and for the next voltages the peak EL intensity continues increasing but within the same order of magnitude.

The plots of the peak and integrated EL intensity with respect to the applied RMS voltage are presented in the semi-logarithmic form in Fig. 6. As can be seen, both plots have the same behavior of a high initial slope just above the threshold voltage (V1 = 25 V) and a rapid saturation above V3 = 38 V. The basic physics of the operation of the device, which occurs when an enough high electric field (above the threshold voltage) is applied across the phosphor, can be explained in terms of four main processes [1]: (1) injection by tunnel emission of electrons from the phosphor/insulator interface, (2) acceleration of electrons to high energies, (3) electron impact excitation of the luminescent centers in the phosphor, and (4) de-excitation of the excited electrons in the luminescent center by radiative or non-radiative recombination. Based on these mechanisms, the increase of the EL intensity with the applied voltage can be directly explained as a result of the increase in the amount and the energy of injected electron, with the consequent increase in the amount of excited and de-excited Mn^{2+} luminescent centers. This also explains the saturation of the EL device at the highest voltages, as the situation where almost all the luminescent centers in the phosphors have been excited. It is important to note that the high initial slope of EL intensity vs voltage observed in the plots of Fig. 6 is indicative of a high device efficiency. Although in this work we could not measure the EL efficiency of these devices, another indicative of their high efficiency is that their EL emission above the threshold voltage could be observed with the naked eye under ambient illumination. In consistency with this, there were not important heating effects on the device, which means a low rate of non-radiative recombination of the excited Mn^{2+} luminescent centers in these devices. The threshold voltage of these EL devices is relatively low compared with those reported previously for optimized MISIM EL devices. Here it is also worth to mention that these ACTFEL were stable and reproducible from one test area to the next.

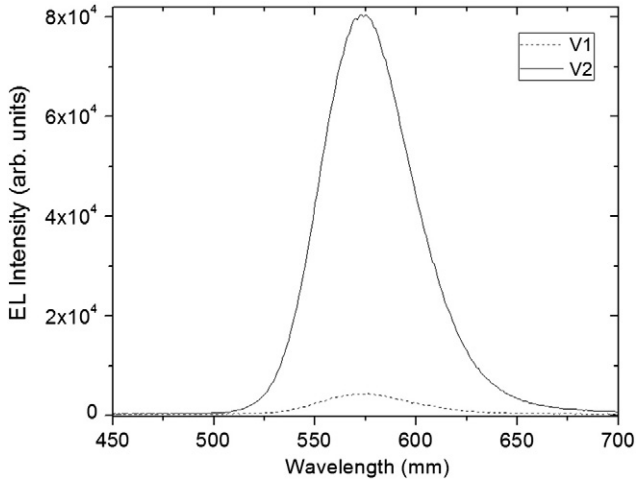

Fig. 4. EL spectra the MISIM structure prepared by ultrasonic spray pyrolysis, with ZnS:Mn film as a phosphor layer, for the threshold RMS voltage V1 = 25 V, and V2 = 32 V. The intense of the peak is 4.4×10^3 (a.u.) and 8×10^4 (a.u.), respectively.

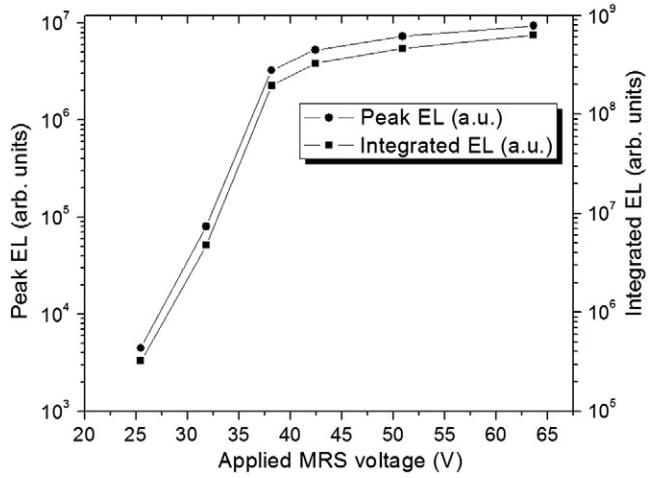

Fig. 6. Peak EL and integrated EL versus RMS voltage plots, for the MISIM structure all-prepared by ultrasonic spray pyrolysis.

4. Conclusions

In summary, MISIM — alternating current thin film electroluminescent devices have been all-fabricated by ultrasonic spray pyrolysis, using ZnO:Al as transparent conducting layer, Al_2O_3 as insulating layers and ZnS:Mn as the semiconductor phosphor layer. The EL intensity vs voltage characteristics of these MISIM EL devices, show a low threshold operation RMS voltage, a high slope and rapid saturation. These results indicate that these MISIM devices prepared by this simple and cheap technique have potential to compete with similar devices fabricated by other standard and more expensive vacuum-deposition techniques.

Acknowledgments

We want to thank to A. Tejeda for X-ray diffraction support and J. Camacho and J.M. García-León for technical assistance.

References

[1] P.D. Rack, P.H. Holloway, Mater. Sci. Eng. R: Rep. 21 (1998) 171.
[2] J.H. Kim, K.H. Yoon, J. Korean Phys. Soc. 56 (2010) 1861.
[3] E.I. Anila, M.K. Jayaraj, J. Lumin. 130 (2010) 2180.
[4] S.J. Wakeham, C. Tsakonas, W.M. Cranton, M.J. Thwaites, G. Boutaud, D.C. Koutsogeorgis, Semicond. Sci. Technol. 26 (2011) 045016.
[5] K.L. Chopra, S. Major, D.K. Pandya, Thin Solid Films 102 (1983) 1.
[6] L. Castañeda, Mater. Sci. Appl. 02 (2011) 1233.
[7] J.F. Wager, J.C. Hitt, B.A. Baukol, J.P. Bender, D.A. Keszler, J. Lumin. 97 (2002) 68.
[8] C. Munasinghe, J. Heikenfeld, R. Dorey, R. Whatmore, J.P. Bender, J.F. Wager, A.J. Steckl, IEEE Trans. Electron Dev. 52 (2005) 194.
[9] C.B. Thomas, W.M. Cranton, Appl. Phys. Lett. 63 (1993) 3119.
[10] K.E. Waldrip, J.S. Lewis, Q. Zhai, M. Puga-Lambers, M.R. Davidson, P.H. Holloway, S.-S. Sun, J. Appl. Phys. 89 (2001) 1664.
[11] A.N. Krasnov, P.G. Hofstra, Prog. Cryst. Growth Charact. Mater. 42 (2001) 65.
[12] M.K. Jayaraj, C.P.G. Vallabhan, Bull. Mater. Sci. 14 (1991) 49.
[13] J.M. Hurd, C.N. King, J. Electron. Mater. 8 (1979) 879.
[14] M.K. Jayaraj, C.P.G. Vallabhan, J. Phys. D: Appl. Phys. 23 (1990) 1706.
[15] J.W. Li, Y.K. Su, M. Yokoyama, J. Electron. Mater. 21 (1992) 659.
[16] M.D. Bhise, M. Katiyar, A.H. Kitai, J. Appl. Phys. 67 (1990) 1492.
[17] T. Minami, T. Utsubo, T. Miyata, Y. Suzuki, Thin Solid Films 445 (2003) 377.
[18] V. Wood, J.E. Halpert, M.J. Panzer, M.G. Bawendi, V. Bulovic, Nano Lett. 9 (2009) 2367.
[19] C. Falcony, M. Garcia, A. Ortiz, J.C. Alonso, J. Phys. D. Appl. Phys. 72 (1992) 1525.
[20] M. Garcia, J.C. Alonso, C. Falcony, A. Ortizl, J. Phys. D: Appl. Phys. 28 (1995) 223.
[21] A. Ortiz, J.C. Alonso, V. Pankov, J. Mater. Sci.: Mater. Electron. 10 (1999) 503.
[22] S.M. Rozati, S. Akesteh, Mater. Charact. 58 (2007) 319.
[23] S.M. Rozati, Can. J. Phys. 86 (2008) 379.
[24] L. Castañeda, R. Silva-González, J.M. Gracia-Jiménez, M.E. Hernández-Torres, M. Avendaño-Alejo, C. Márquez-Beltrán, M. de la L. Olvera, J. Vega-Pérez, A. Maldonado, Mater. Sci. Semicond. Process. 13 (2010) 80.
[25] A. Ortiz, J. Alonso, V. Pankov, D. Albarran, J. Lumin. 81 (1999) 45.
[26] A. Ortiz, J.C. Alonso, V. Pankov, A. Huanosta, E. Andrade, Thin Solid Films 368 (2000) 74.
[27] A. Ortiz, J.C. Alonso, J. Mater. Sci.: Mater. Electron. 13 (2002) 7.
[28] M. Garcia sanchez, J. Peña, A. Ortiz, G. Santana, J. Fandiño, M. Bizarro, F. Cruz-Gandarilla, J. Alonso, Solid State Ionics 179 (2008) 243.
[29] H. Yang, Z. Wang, L. Song, M. Zhao, Y. Chen, K. Dou, J. Yu, L. Wang, Mater. Chem. Phys. 47 (1997) 249.
[30] L. Cao, J. Zhang, S. Ren, S. Huang, Appl. Phys. Lett. 80 (2002) 4300.
[31] R. Maity, K.K. Chattopadhyay, Nanotechnology 15 (2004) 812.
[32] M.H. Yousefi, A.A. Khosravi, K. Rahimi, A. Nazesh, Eur. Phys. J. Appl. Phys. 45 (2009) 10602.
[33] M. Stefan, S.V. Nistor, D. Ghica, C.D. Mateescu, M. Nikl, R. Kucerkova, Phys. Rev. B 83 (2011) 045301.